

# Performance of Static Voltage Stability Analysis in MATLAB Environment with Further Applications

Jan Veleba<sup>(1)</sup>, Tomas Nestorovic<sup>(2)</sup>

Department of Electric Power Engineering and Environmental Engineering<sup>(1)</sup>  
New Technologies for the Information Society<sup>(2)</sup>  
University of West Bohemia in Pilsen  
Pilsen, Czech Republic, EU  
jveleba@kee.zcu.cz<sup>(1)</sup>, nestorovic@ntis.zcu.cz<sup>(2)</sup>

**Abstract**— Nowadays, electric power systems have been often operated close to their feasible limits due to increased electric power consumptions, large installments of renewable power sources, and deliberated power market policies. These pose a serious threat to stable network operation and control. Therefore, both static and dynamic voltage stabilities are currently one of the key topics worldwide for preventing related black-out and islanding scenarios. In this paper, modelling and simulations of static voltage stability problems in MATLAB environment are performed using author-developed computational tool implementing both conventional and more advanced numerical approaches. Their performances are compared with Simulink-based library Power System Analysis Toolbox (PSAT) in terms of solution accuracy, CPU time and possible limitations. Furthermore, their use for locating critical network buses/branches/areas and most critical loading scenarios in terms of voltage stability are demonstrated. Eventually, their both real-time and off-line monitoring and assessment capabilities of system's voltage stability are also discussed.

**Index Terms**—Static voltage stability, continuation load flow analysis, predictor-corrector method, voltage stability margin, voltage-power sensitivity, shortest distance to voltage instability, voltage stability indices, Power System Analysis Toolbox.

## I. INTRODUCTION

Static voltage stability is defined as the capability of the system to withstand a small disturbance (e.g. fault occurrence, small change in parameters, topology modification, etc.) without abandoning a stable operating point [1]-[5]. Voltage stability problems are generally bound with long 'electrical' distances between reactive power sources and loads, low source voltages, severe changes in system topology, and low level of var compensation. However, this does not strictly mean that voltage instability is directly connected only with low-voltage scenarios. Also, broad variety of practical situations can eventually lead to voltage collapse, e.g. tripping a parallelly connected line during the fault, reaching the var limit of a synchronous generator/condenser, restoring low supply voltage in induction motors after the fault. All of these cause the reduction of vars for supporting bus voltages which

results in increases of branch currents, further voltage drops, and lower var flows until the voltage collapse occurs. This entire process may appear in time from seconds to even tens of minutes.

To prevent voltage collapse scenarios, several types of compensation devices are massively used worldwide - both shunt capacitors/inductors, series capacitors, SVCs, synchronous condensers, STATCOMs, etc. Moreover, other principles can be applied, e.g. reconfigurations (connecting parallel lines/cables/transformers), power transfer limitations, activations of new generating units, under voltage load shedding of low-priority loads. However, actions of OLTC transformers must be blocked during low voltage stability events since each tap position corresponds to an increase of the load which eventually leads to higher branch losses and further voltage drops [1]-[2], [4].

Static voltage stability problem is becoming very popular these days due to many real black-out occurrences emerging currently around the world. This interest can be well documented on large number of research papers. In [6], the Monte Carlo approach is employed to evaluate specialized indices of the power system for finding the weakest network bus in terms of voltage stability. Novel method [7] consists of the repetitive load flow computation with gradually increasing system loading but replacing the original load flow approach by the time simulation concept. Wu elimination method [8] is applied for obtaining analytical load flow solutions, V-P and V-Q curves and static voltage stability margins. Authors in [9] use the L-index technique to calculate voltage stability margins and locate the weak areas of the network while the trained ANN is applied to predict the values of important system control quantities. In [10], evolutionary programming technique is applied for finding the maximum loadability point for a single or multiple bus load increase. Approach in [11] applies the particle swarm optimization algorithm for finding the shortest distance to instability by determining the most critical system loading scenario. Fast method for obtaining static voltage stability region by using the combination of the loop current and the node voltage method is introduced in [12].

New method [13] is proposed for solving the voltage stability problem of radial distribution networks by means of the backward/forward method with Thévenin's equivalent circuit identification.

This paper is organized as follows. Sections II and III describe author-developed codes for the conventional Cycled Newton-Raphson (CNR) method and more robust Continuation Load Flow (CLF) method to perform the voltage stability analysis, respectively. Independent tool - Power System Analysis Toolbox (PSAT) - is briefly introduced in Section IV. In Sections V and VI, theoretical background for advanced voltage stability problems, i.e. locating weak network buses/branches/areas and determining the shortest distances to voltage instability (so-called SDVI analysis), is briefly covered. In Section VII, key properties of both of author-developed CNR and CLF codes are discussed. Sections VIII and IX show the basic voltage stability results for broad variety of test power systems. Key case studies for both advanced stability problems are presented in Sections X and XI. Finally, Section XII evaluates each of the techniques applied and provides transparent conclusion of this paper.

## II. CONVENTIONAL NUMERICAL CALCULATION OF THE VOLTAGE STABILITY PROBLEM

When increasing the loading (or loadability factor  $\lambda$ ) of the system, its bus voltages slowly decrease due to the lack of reactive power. At the singular point, characterized by maximum loadability factor  $\lambda_{\max}$  and critical bus voltages, the system starts to be unstable and voltage collapse appears. From this point on, only lower loading with low voltage values lead to the solution. The dependence between bus voltage magnitudes and  $\lambda$  is graphically represented by the V-P curve, sometimes also referred to as the nose curve. Unfortunately, initial (base-case) position of the system operating point on the V-P curve is not known along with its distance from the voltage collapse (i.e. voltage stability margin). Thus, location of the singular point must be found during the analysis.

Note: Values of  $\lambda_{\max}$  and critical voltages are rather theoretical since they do not reflect voltage/flow limits of network buses/branches. When incorporating these practical restrictions, the real maximum loadability  $\lambda_{\max}^*$  can be found for keeping all bus voltages and branch loadings within limits.

Traditional approach for finding the maximum system loadability is to apply the standard Newton-Raphson (N-R) method for the base-case load flow calculation (i.e. for  $\lambda = 1.0$ ). When obtaining current position on the V-P curve, network loading (i.e. loads/generations in selected network buses) is increased in defined manner by a certain step and the load flow is computed repetitively along with a new position on the V-P curve. This process continues in an infinite loop until the singular point is reached. However, total number of iterations in each V-P step is gradually increasing so that when close to the singular point, the N-R method fails to converge, i.e. no solution is provided. This relates to the fact that Jacobian  $\underline{J}$  becomes singular (i.e.  $\det \underline{J} \approx 0$ ) and its inverse matrix cannot be computed for keeping numerical convergence.

To speed up the calculation, variable step change is applied. Usually, a single step value is used. When obtaining the divergence of the N-R method, the step size is simply divided by two and the calculation for the current V-P point is repeated until the convergence is achieved. When the current step size value reaches the predefined minimum value, the calculation is stopped. Despite of the relatively simple procedure, the CNR method enables the completion of the stable V-P curve only. Unstable part including the singular point cannot be examined. Also, high CPU requirements prevent this method from being employed for larger power systems.

In this paper, the CNR algorithm was developed and further tested on wide range of test power systems.

## III. CONTINUATION LOAD FLOW ANALYSIS

CLF analysis [1], [14] suitably modifies conventional load flow equations to become stable also in the singular point. Eventually, both upper/lower parts of the V-P curve can be drawn. It uses a two-step predictor/corrector algorithm along with the new unknown state variable called continuation parameter (CP). Predictor (Eq. 1) is a tangent extrapolation of the current operation point estimating approximate position of the new point on the V-P curve.

$$\begin{bmatrix} \theta \\ V \\ \lambda \end{bmatrix}^{\text{predicted}} = \begin{bmatrix} \theta_0 \\ V_0 \\ \lambda_0 \end{bmatrix} + \sigma \begin{bmatrix} \vdots & \vdots & \vdots \\ \underline{J} & \vdots & K \\ \vdots & \vdots & \vdots \\ \dots & \dots & \dots \\ e_k & \dots & \dots \end{bmatrix}^{-1} \begin{bmatrix} 0 \\ \vdots \\ 0 \\ 1 \end{bmatrix} \quad (1)$$

Vector  $K$  contains base-case power generations and loads. Variables  $\theta_0$ ,  $V_0$ ,  $\lambda_0$  define the system state from the previous corrector step. Vector  $e_k$  is filled with zeros and certain modifications (see [1], [14]) are implemented for selected CP in each network bus  $k$  at the current point on the V-P curve. Remaining elements in Eq. 1 are the newly computed Jacobian  $\underline{J}$  and step size  $\sigma$  of the CP.

Tangent predictor is relatively slow, anyway shows good behaviour especially in steep parts of the V-P curve. Unlike tangent predictor, secant predictor is simpler, computationally faster, and behaves well in flat parts of the V-P curve. In steep parts (i.e. close to the singular point and at sharp corners when a generator exceeds its var limit) it computes new predictions too far from the exact solution. This may eventually lead to serious convergence problems in the next corrector step. Thus, tangent predictor is more recommended to be applied.

Corrector is a standard N-R algorithm for correcting state variables from the predictor step to satisfy load flow equations. Due to one extra parameter  $\lambda$ , additional condition (Eq. 2) must be included for keeping the value of the CP constant in the current corrector step. This condition makes the final set of equations non-singular even at the bifurcation point.

$$x_k - x_k^{\text{predicted}} = 0, \quad x = \begin{cases} \lambda & \text{if CP is } \lambda \\ V & \text{if CP is } V \end{cases} \quad (2)$$

For the CP, state variable with the highest rate of change must be chosen (i.e.  $\lambda$  and  $V$  in flat and steep parts of the V-P curve, respectively). If the process diverges, parameter  $\sigma$  must be halved or parameter CP switched from  $\lambda$  to  $V$ .

Difference between both types of predictors and the entire process of the predictor/corrector algorithm is demonstrated in Fig. 1. Horizontal/vertical corrections are performed with respect to chosen CP type.

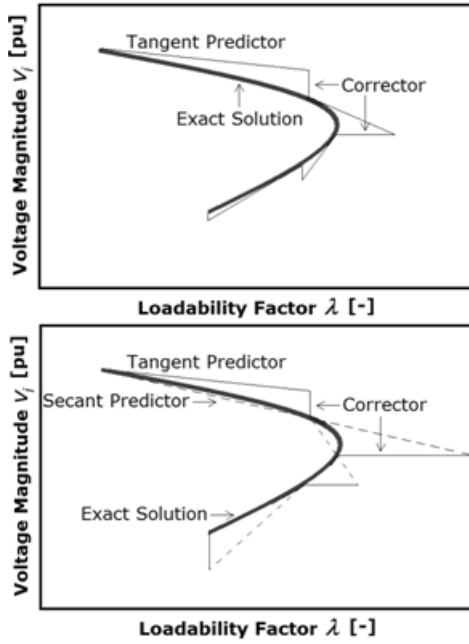


Fig. 1. Predictor/Corrector Mechanism for CLF Analysis [15].

Step size should be carefully increased to speed up the calculation when far from the singular point, or decreased to avoid convergence problems when close to the peak. Step size modification based on the current position on the V-P curve (i.e. as a function of the line slope for previous two corrected points on the V-P curve) is recommended in [16]. This approach belongs to so-called rule-based or adaptive step size control algorithms. For more, please, see Section VII.

CLF analysis still remains very popular for high-speed solving of voltage stability studies. Due to its reliable numerical behaviour, it is often included into the N-R method providing stable solutions even for ill-conditioned load flow cases. Moreover, it is applied in foreign control centres for N-1 on/off-line contingency studies with frequencies of 5 and 60 minutes [2], respectively.

#### IV. POWER SYSTEM ANALYSIS TOOLBOX (PSAT)

PSAT [17] is a Simulink-based open-source library for electric power system analyses and simulations, distributed via General Public License (GPL). It contains the tools for load

flow (busbars, lines, two-/three-winding transformers, slack bus(es), shunt admittances, etc.), CLF and OPF data (power supply/demand bids and limits, generator power reserves and ramping data), small signal stability analysis and time domain simulations. Moreover, line faults and breakers, various load types, machines, controls, OLTC transformers, FACTS and other can be also modelled. User-defined device models can be added as well.

All studies must be formulated for one-line network diagram only - either in input data \*.m file in required format or in graphical \*.mdl file containing manually drawn network scheme. For the former option, input data conversions from and to various common formats are available (e.g. PSS/E, DlgSILENT, IEEE cdf, NEPLAN, PowerWorld and others).

When compared to another MATLAB-based open-source tool MATPOWER [18], PSAT is more efficient and highly advanced by providing more analyses, problem variations, possible outputs and other useful features in its user-friendly graphical interface. MATPOWER does not support most of advanced network devices, entirely omits CLF analysis and has neither graphical user interface nor graphical network construction ability. Also, it does not consider var limits in PV buses at all. Incorrect interpretation of reactive power branch losses can be also observed.

#### V. IDENTIFICATION OF CRITICAL NETWORK REGIONS IN TERMS OF VOLTAGE STABILITY

For comprehensive voltage stability analysis, several voltage stability margin indices were developed in the literature for finding the most critical buses/branches/areas of the system. In these regions, preventive or remedial actions should be taken with the highest priority.

Voltage stability margin indices (VSMI) [4], [5], [16] express percentage distance of base-case bus voltage magnitudes from their critical values - see Eq. 3. Those buses with very low absolute VSMI values are too close to the voltage collapse.

$$VSMI_i = (V_{i(\lambda=1)} - V_{i(\lambda=\lambda_{\max})}) / V_{i(\lambda=\lambda_{\max})} \times 100\% \quad (3)$$

Similar indices for branch angular displacements can be also defined [5]. Comparing base-case and critical angular values, the formula is as follows.

$$VSMI_{ik} = (\theta_{ik(\lambda=\lambda_{\max})} - \theta_{ik(\lambda=1)}) / \theta_{ik(\lambda=\lambda_{\max})} \times 100\% \quad (4)$$

It is impossible to automatically presume that all PV buses will be switched to PQ before the bifurcation point. Many buses may still preserve their var compensation ability due to broad var limits or low local transfers of reactive power. Therefore, relative reactive power reserve [19] should be also assessed at every point of the V-P curve - see Eq. 5.

$$q_{\text{reserve}} = 1 - \sum_i^{PV} Q_{Gi} / \sum_i^{PV} Q_{Gi \max} \quad (5)$$

VSMI values show the voltage proximities to the collapse point without any dynamics. Therefore, voltage-load bus sensitivities or voltage sensitivity factors (VSF) [1], [5] should be also calculated - see Eq. 6. Elements  $dV$  are the voltage increments computed by the tangent predictor (Eq. 1) in the singular point or its close vicinity.

$$VSF_i = dV_i / \sum_{k=1}^n dV_k \quad (6)$$

Note: The norm of tangent increments  $dV$  and  $d\theta$  can be used as an additional index for saddle-node proximity prediction as well.

Individual factors/indices show only one half of the information needed. When combined, clearer picture about the system status can be seen. Therefore, collective evaluation of all these voltage stability indices and sensitivity factors should be applied for more detailed voltage stability assessment of the electric power system. For example, voltage stability is especially critical for those buses with very low VSMI values but very high VSF values. Such buses and those with negative sensitivities (unstable operation) should be primarily corrected.

#### VI. SHORTEST DISTANCE TO VOLTAGE INSTABILITY PROBLEM

Voltage stability margin, i.e. the distance to voltage instability, is usually evaluated by stressing the system loading in certain predefined manner (with constant power factor, most probable scenario based on historical/forecasted data). However, it is also important to determine such loading pattern for all non-slack network buses, which results in the minimum stability margin. Then, such set of MW/MVAr bus increments has the minimum vector sum and causes the Jacobian to be singular when added to the base-case loading.

One of the methods [1] is further explained on a simple 2-bus power system containing the PQ bus No. 2 with connected initial P-Q load. The aim is to find such loading scenario for  $P_{L2}$  and  $Q_{L2}$  which leads to minimum distance to black-out. In a P-Q 2D plane (see Fig. 2), initial loading  $(P_{L0}, Q_{L0})$  can be projected. Curve  $S$  connects the load cases for which the Jacobian is singular and voltage instability occurs. All points inside the area and out of it represent stable and unstable voltage conditions, respectively. For higher-dimensional cases, curve  $S$  turns to a general hypersurface.

Principle of the method is to increase the load from initial conditions in some chosen direction until voltage instability appears (point ①). The normal to curve  $S$  in this point (vector  $\eta_1$ ) is determined representing the new direction for initial load change. Thus, the system is stressed again from initial conditions with new loading scenario  $\eta_1$  and new point ② on the curve  $S$  is reached. Loading scenario is updated by computing the normal to curve  $S$  ( $\eta_2$ ). The process is iteratively repeated until convergence to the solution (shortest distance to instability) is obtained (point ⑤). In such case, the normal is exactly parallel to applied loading scenario direction. This method seems to be relatively simple and fast-converging.

For an arbitrarily large power system, mathematical model of this method considers the increase of active/reactive power loads in PQ buses and active power generations in PV buses. Then, the N-R's Jacobian  $J$ , state vector  $x = [\theta; V]$  and parameter vector  $\rho = [P; Q]$  have identical sizes, i.e.  $n_{PQPV} = 2n_{PQ} + n_{PV}$ . Note: Increase of active/reactive power loads and active power generations is considered only in those buses where real loads/generations are physically connected. The entire procedure is as follows:

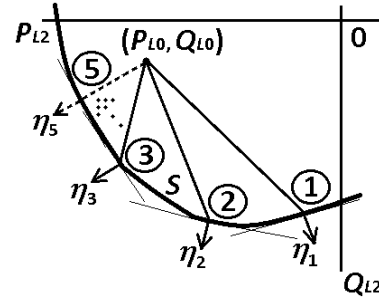


Fig. 2. Principle of the method.

1) The system is activated for initial load/generation stressing, i.e.  $i = 0$ . As the initial load/generation stressing, direction vector  $\eta_i$  with constant power factor (or equal increase rate) is recommended. Direction vector  $\eta_i$  is then normalized, i.e.  $|\eta_i| = 1$ .

2) The system is stressed from the initial system operating point  $(x_0, \rho_0)$  incrementally along a chosen direction  $\eta_i$ . Load/generation increase is defined as:

$$\rho_i = \rho_0 + k_i \eta_i \quad (7)$$

3) Stressing is stopped when reaching the voltage stability singular point  $(x_i^*, \rho_i^*)$ . The system is on the surface  $S$  and the Jacobian  $J$  is close to be singular. It applies:

$$\rho_i^* = \rho_0 + k_i \eta_i \quad (8)$$

4) Distance to voltage instability  $k_i$  can be evaluated by the norm.

$$k_i = |\rho_i^* - \rho_0| \quad (9)$$

5) If the difference between two newly computed values of  $k_i$  falls below a pre-set convergence criterion ( $1 \times 10^{-8}$ ), the procedure is stopped and the shortest distance to instability  $k_i^*$  is found. Otherwise, continue with step 6).

6) The left eigenvector  $w_i$  corresponding to zero real eigenvalue of singular matrix  $J$  is obtained. Index  $i$  is increased by 1 and the new direction vector  $\eta_i$  is calculated.

$$\eta_i = w_i \quad \text{and} \quad |\eta_i| = 1 \quad (10)$$

7) Move back to 2).

Using this procedure, the shortest distance to instability  $k_i^*$  can be found. For such point applies:

$$\rho_i^* = \rho_0 + k_i^* \eta_i^* \quad (11)$$

Minimum load/generation increases ( $k_i^* \eta_i^* = \rho_i^* - \rho_0$ ) are also obtained for all network buses providing the most critical loading scenario for reaching the singular point.

For this methodology, several key ideas must be kept in mind. 1] Hypersurface  $S$  is to be completely smooth. However, this is not valid for PV buses with var limits. Therefore, possible actions of bus-type switching logics must be prevented. 2] Hypersurface  $S$  in the parameter space has an unknown shape. Therefore, only a local minimum dependent on the initial direction of load/generation stressing can be found. Therefore, an experienced guess based on measured/forecasted network operation should be employed to obtain a reasonable critical scenario. 3] Only the generators are assumed to be connected to PV buses, i.e. no loads in PV buses are considered.

In this paper, presented optimization method was programmed and applied for load-only power systems (distribution networks, grids with no PV buses) using the modified CNR method. The goal was to provide sufficiently reliable and fast solutions since no professional software provides this type of voltage stability analysis and only a few pieces of literature are devoted to this problem.

#### VII. PROPERTIES OF AUTHOR-DEVELOPED CNR AND CLF CODES IN MATLAB ENVIRONMENT

As previously shown, there already exists a MATLAB-based application that meets the requirements for static voltage stability analysis of electric power systems. Due to its several limitations and CPU time restrictions (see Section IX), our goal was to focus primarily on speed/precision improvements of voltage stability studies. Therefore, a specialized tool in MATLAB environment was developed using both CNR and CLF routines for providing fundamental examination of medium-sized and larger power systems in terms of static voltage stability. Several key aspects of these codes are discussed below.

1] Predictor: Despite of computationally more expensive algorithm, tangent predictor was used for finding reliable estimations of new V-P points especially around the singular point. Applied in CLF algorithm only.

2] Corrector: First, corrector step is used at the start of the CLF program to find the base-case point for further calculations. Due to possible weak numerical stability at this point (for badly-scaled power systems), the One-Shot Fast-Decoupled (OSFD) procedure is implemented to the standard N-R method for providing more stable solutions and thus preventing numerical divergence. Moreover, voltage truncation (SUT algorithm) is also included into the state update process at every N-R's iteration. Both of these stability approaches were examined and further tuned in [20]. They were also

applied to CNR algorithm to increase the loading range for which the stable load flow solutions can be obtained. Thus, closer proximity to singular point can be reached.

3] Step size: Largest-load PQ network bus is chosen for computing the angle  $\alpha$  between the horizontal and the line interconnecting two adjacent V-P points. Based on this, step size evaluation function (Eq. 12) is applied - see Fig. 3.

$$\sigma = \begin{cases} \sigma_L & \text{for } |\alpha| \geq \pi/8 \\ \sigma_U & \text{for } |\alpha| \leq \pi/32 \\ A/\sin^2 \alpha + B & \text{otherwise} \end{cases} \quad (12)$$

The upper and lower step limit constants  $\sigma_U$  and  $\sigma_L$  define the step size for the flat part of the V-P curve and for close vicinity to the singular point, respectively.

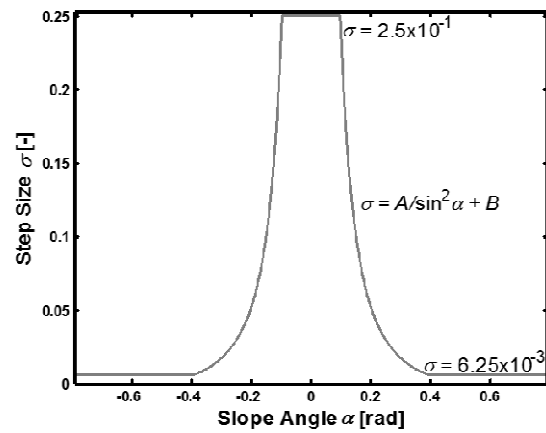


Fig. 3. Step size evaluation function [15].

For the CNR algorithm, this is a rather too complex concept of step size control. Therefore, only a single step size is chosen at the start and a simple step-cutting technique (dividing by 2) is applied in case of divergence.

4] Ending criterion: Only stable part of the V-P curve (incl. exact singular point calculation) is computed by CLF code. Thus, if the computed value of  $\lambda$  begins to decrease, the process is stopped. For the CNR code, the calculation is terminated when the step size falls below a given small value (e.g.  $1 \times 10^{-8}$ ). For each load flow case, maximum number of iterations and permitted tolerance for convergence is set to 20 and  $1 \times 10^{-8}$ , respectively.

5] Calculation speed and accuracy: For excessively accurate voltage stability solutions, values of  $2.5 \times 10^{-2}$  and  $6.25 \times 10^{-4}$  are used for constants  $\sigma_U$  and  $\sigma_L$  in the CLF algorithm. Rather compromise values of  $5 \times 10^{-2}$  and  $1 \times 10^{-2}$  can be used to obtain fast and fairly accurate solutions for any of tested power systems. For the CNR algorithm, initial step size of  $2.5 \times 10^{-2}$  seems to be sufficient enough.

6] Code versatility: Both CNR and CLF procedures are programmed so that the user directly specifies an arbitrary group of network buses for load/generation increase. From this

set of buses, only those non-slack buses with non-zero active power loads/generations are involved into the analysis. For simplicity, load/generation increase in the entire network was considered in each of studies performed, i.e. all network buses were always selected.

Two scenarios can be activated by the user. a) L scenario increases both P/Q loads in selected PQ/PV buses with constant power factor (i.e. with identical increase rate). b) L+G scenario increases both P/Q loads in selected PQ/PV buses and P generations in selected PV buses (with identical increase rate).

7) Var limits: In both approaches, bus-type switching logics are applied to iteratively computed reactive powers  $Q_{Gi}$  in PV buses when exceeding the var limit (Eq. 13), or to relevant bus voltages when returning the vars back inside the permitted var region (Eq. 14).

$$Q_{Gi} = \begin{cases} Q_{Gi \max} & \text{if } Q_{Gi} > Q_{Gi \max} \\ Q_{Gi \min} & \text{if } Q_{Gi} < Q_{Gi \min} \end{cases} \quad (13)$$

$$V_i = V_i^{sp} \text{ if } \left\{ \begin{array}{l} Q_{Gi} = Q_{Gi \max} \text{ AND } V_i > V_i^{sp} \\ \text{OR} \\ Q_{Gi} = Q_{Gi \min} \text{ AND } V_i < V_i^{sp} \end{array} \right\} \quad (14)$$

Variables  $Q_{Gi \max}$  and  $Q_{Gi \min}$  are the upper and lower var limits while  $V_i^{sp}$  determines the specified value of voltage magnitude for each PV bus.

8) Code limitations: a) With increased loading, lower/upper var limits in PV buses should not be fixed but vary proportionally to the generated active power. In both codes, constant var limits are used for more pessimistic V/Q control. b) Only identical increase rate is applied. However, implementing user-defined increase rates for each generation/load would not pose any serious problems to developed codes.

9) Outputs: Theoretical value of  $\lambda_{\max}$  and  $V-\lambda$  data outputs for V-P curves are computed and stored or graphically projected. Respective values of  $\lambda$  for switching some of PV buses permanently to PQ are also recorded. Voltage and power flow limits were not considered for the evaluation of real maximum loadability  $\lambda_{\max}^*$ .

10) Sparse programming: Sparsity techniques along with smart vector/matrix programming are used in both CNR and CLF codes to significantly decrease the CPU time needed for each load flow case.

### VIII. TESTING OF CNR AND CLF ALGORITHMS FOR SOLVING VOLTAGE STABILITY LOAD FLOW PROBLEMS

Total number of 50 test power systems between 3 and 734 buses were analyzed using developed CNR and CLF algorithms in MATLAB environment. Identical increase rate was applied to all network buses (before filtering those with non-zero active power loads or generations). For both L and L+G scenarios, only stable part of the V-P curve was

calculated with var limits included. Settings of both codes are as introduced in Section VII, Paragraphs 4 and 5. In Table I., voltage stability solutions of several test cases are shown. Presented results contain the maximum loadability, numbers of stable V-P points, and CPU times in seconds needed. For each of the cases, the first two rows show the outputs of the CLF code for excessive and compromise accuracy, respectively. As the comparison, the third row provides the results of the CNR code.

As can be seen, exact solutions of maximum loadability were obtained for both of tested methods and each of the three accuracy settings. The first setting was apparently too much focused on producing exact results. Therefore, numbers of V-P points and CPU times often exceeded 200 and 1 second, respectively. When using fair compromise setting, the maximum error for  $\lambda_{\max}$  from all 50 test power systems was only 0.0185 percent, while numbers of points and CPU times were decreased on average by 75.27 percent and 64.11 percent, respectively.

TABLE I. VOLTAGE STABILITY SOLUTIONS USING CNR AND CLF ALGORITHMS - L AND L+G SCENARIOS

Case	Scenario L			Scenario L+G		
	$\lambda_{\max}$ [-]	points	time [s]	$\lambda_{\max}$ [-]	points	time [s]
IEEE9	1.302632	331	0.5616	1.162053	215	0.3900
	1.302632	27	0.1404	1.162052	24	0.1248
	1.302632	23	0.4056	1.162053	20	0.4212
IEEE14	1.760331	658	1.2012	1.777995	506	0.9360
	1.760331	87	0.2340	1.777995	59	0.2028
	1.760331	43	0.5460	1.777995	45	0.6396
IEEE30	1.536905	854	1.9500	1.546751	726	1.6536
	1.536905	88	0.2808	1.546752	124	0.4212
	1.536905	37	0.6396	1.546751	37	0.6552
IEEE57	1.406778	891	2.9016	1.616845	399	1.3884
	1.406778	229	0.6864	1.616845	57	0.2652
	1.406778	27	0.8112	1.616845	37	0.8112
IEEE162	1.079959	1640	12.9169	1.138996	1185	9.3913
	1.079960	464	3.1044	1.138996	65	0.8112
	1.079960	13	1.7628	1.138996	16	1.8408
IEEE300	1.024573	8457	103.8655	1.058820	311	4.0092
	1.024573	529	7.0044	1.058819	94	1.4508
	1.024573	16	2.4180	1.058820	17	2.5584
EPS734	3.104162	139	4.5864	3.104162	139	4.8360
	3.104083	46	1.8720	3.104083	46	1.8408
	3.104162	96	8.2369	3.104162	96	8.1745

CNR code obtains highly accurate results in terms of solution accuracy. In majority of cases, it provides even better solutions than CLF algorithm with compromise accuracy. Surprisingly, it always computes slightly higher maximum loadability values than the highly accurate CLF code. This seems to be one of visible drawbacks of CNR method. Only low numbers of V-P points are needed for reaching close proximity to the singular point. These numbers are well comparable to those needed for compromise CLF code. Unfortunately, each divergence case (between 22 and 28) significantly prolongs the entire computation process of the CNR method.

Therefore, the CNR code suffers from being extremely time-dependent on computing each V-P point. When compared

to compromise CLF code, the CPU time needed by the CNR method is on average about 167 percent higher. Therefore, compromise CLF code seems to be the best method for providing fast, reliable, and highly accurate voltage stability results for majority of analyzed power systems.

Stable V-P curves of the IEEE 30-bus power system (L+G scenario) were computed using both CNR and CLF methods, and they are shown in Figs. 4 and 5, respectively. For the CLF method, the V-P curves are extended to demonstrate numerical stability of this algorithm around the singular point. Extensions of V-P curves into the unstable region is provided for  $0.97 \times \lambda_{\max} < \lambda < \lambda_{\max}$ .

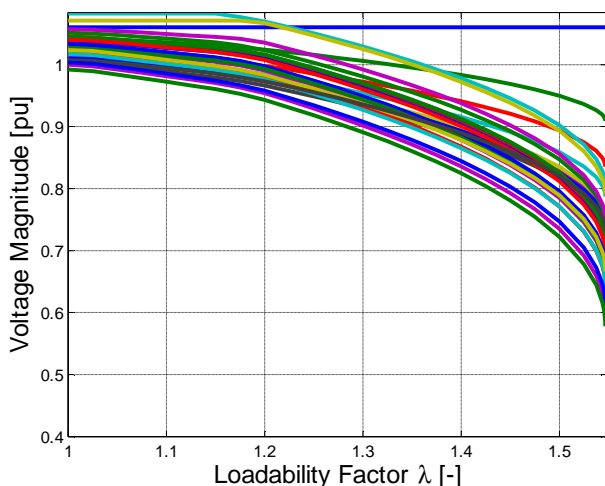


Fig. 4. V-P curves for the IEEE 30-bus system (CNR method).

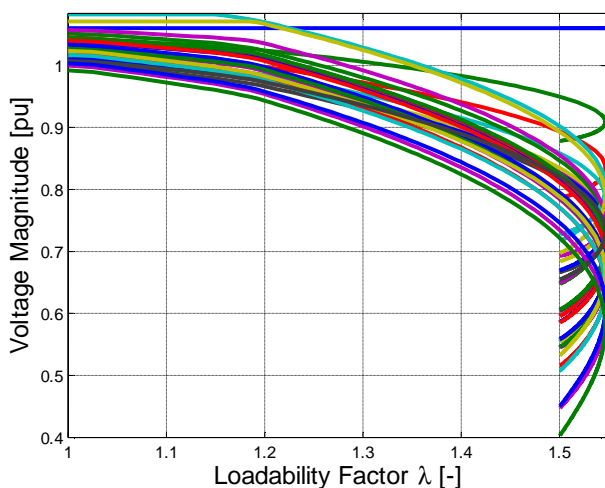


Fig. 5. Extended V-P curves for the IEEE 30-bus system (CLF method).

As Table I. shows, applied version of CLF method is still not applicable for real-time voltage stability monitoring, but it can be useful for off-line reliability, evaluation or planning studies of even larger networks.

### IX. TESTING OF PSAT FOR SOLVING VOLTAGE STABILITY LOAD FLOW PROBLEMS

Despite PSAT has many advantages, it also suffers from several drawbacks. Four of them were spotted during the testing stage when large number of load flow studies was solved using PSAT and results were compared with author-developed N-R code in MATLAB environment. First, inefficient PV-PQ bus type switching logic is applied. Probably, reverse switching logic (Eq. 14) is not used and the need for convergence is requested to activate the forward switching logic (Eq. 13). As the result, unnecessarily more PV buses are being switched permanently to PQ. Furthermore, switching logic completely fails to switch PV buses to PQ for larger systems with high numbers of PV buses. Second, nominal voltages must be always defined in the input data file otherwise the error message 'Divergence - Singular Jacobian' is obtained during the simulation. This seems to be entirely illogical since nominal voltages should not be necessary for the 'in per units defined' problem. Third, it seems that no advanced stability techniques are applied for the N-R method in PSAT because of severe numerical oscillations appearing in several studies. Finally fourth, PSAT intentionally neglects transformer susceptances and thus causes errors in final load flow results. A column for shunt susceptances is available for power lines only. For transformers, this column is reset to zero automatically.

Under these limitations, load flow results show very good congruity between author-developed N-R method and PSAT. Higher total numbers of iterations are needed by PSAT due to missing stability technique(s). Also, CPU times are higher in PSAT due to combining the codes with other analyses and related tool features.

As an example, load flow and voltage stability analysis of the IEEE 14-bus power system is accomplished by PSAT - see Figs. 6-10.

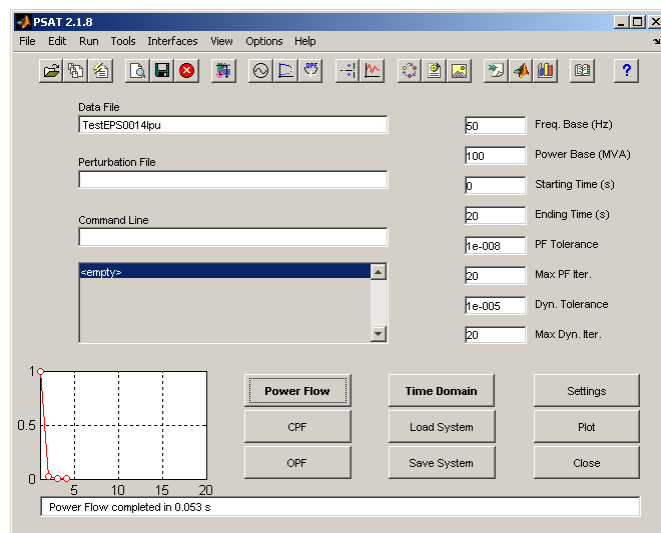


Fig. 6. GUI in PSAT for load flow analysis of IEEE 14-bus system.



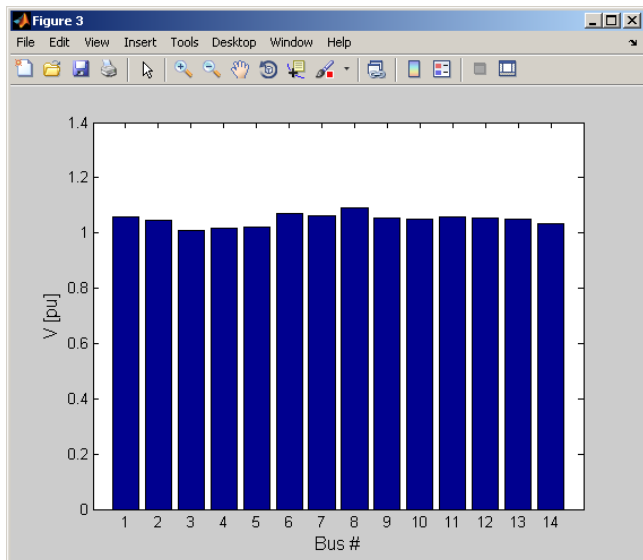


Fig. 7. Final voltage magnitudes of IEEE 14-bus power system in PSAT.

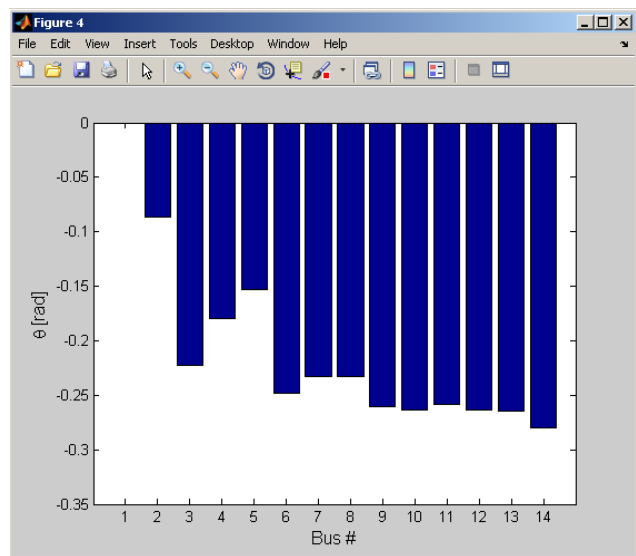


Fig. 8. Final voltage angles of IEEE 14-bus power system in PSAT.

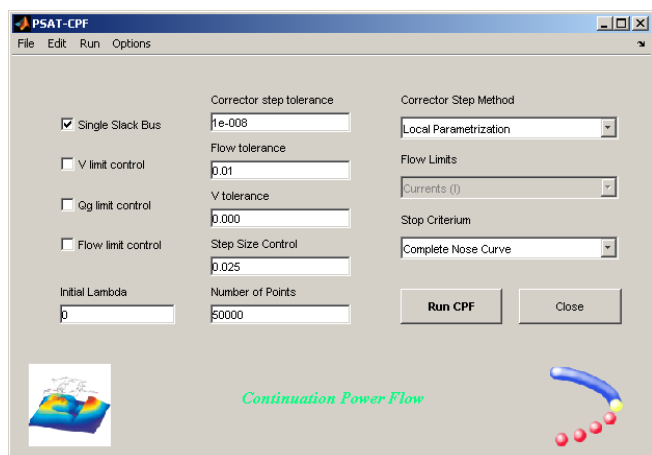


Fig. 9. Settings of CLF code for solving the IEEE 14-bus power system.

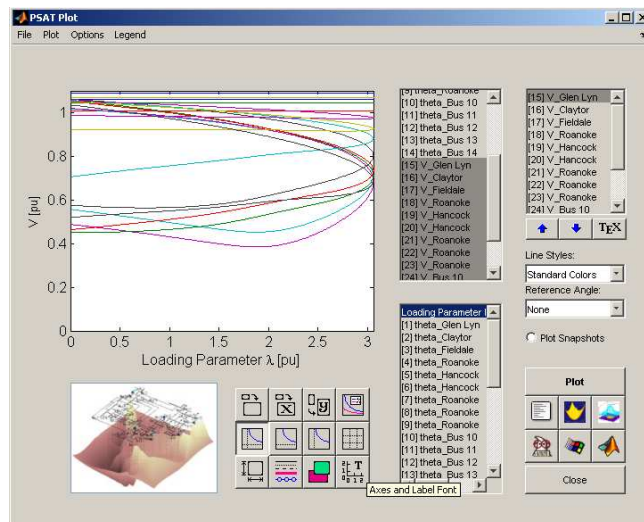


Fig. 10. Nose curves for all network buses of IEEE 14-bus power system.

For voltage stability studies, PSAT contains the advanced CLF algorithm with contingency and OPF analyses. Load flow data are extended by two matrices specifying the sets of PQ/PV buses where the loads/generations are to be increased (different increase rates available). CLF code is then started via specialized window (Fig. 9). Calculation can be adjusted by the user for better computational performance - e.g. by setting more suitable step size, maximum number of V-P points, and by voltage/var/flow control. PSAT offers two CLF methods - perpendicular intersection (PI) and local parametrization (LP). Three stopping criteria are available: Complete Nose Curve (computing both stable/unstable parts of the V-P curve), Stop at Bifurcation (when singular point exceeded) and Stop at Limit (when voltage/flow/point limit reached).

CLF algorithm in PSAT is defined so that power increases are realized by adding a power increment (loadability factor multiplied by increase rate) to the base-case loading, i.e. initial  $\lambda$  is zero. In author-developed CNR and CLF codes, power increases are performed by multiplying the base-case loading with  $\lambda$ . Therefore, maximum loadability in PSAT must be increased by unity when comparing both software tools. In Table II., voltage stability solutions for medium-sized IEEE test systems are provided by the author-developed CNR and compromise CLF codes when compared to those obtained by PSAT (PI mode with step 0.025 and LP mode with default step 0.5). As the outputs, theoretical values of  $\lambda_{max}$ , numbers of stable V-P points and CPU times were stored. For all voltage stability studies in PSAT, identical power increase rates (L+G scenario) were applied with deactivated logics for var limits.

Both of PSAT modes showed only average accuracy with satisfiable numbers of V-P points and lower computing speed. LP mode was more time-consuming but needed lower numbers of V-P points and usually provided more accurate results. Compromise CLF code provided the best combination of solution accuracy and CPU time in all the cases. Higher numbers of V-P points were needed but CPU times were still rather smaller than those in PSAT due to optimized sparse programming applied.



TABLE II. VOLTAGE STABILITY ANALYSIS OF MEDIUM-SIZED IEEE TEST SYSTEMS (AUTHOR-DEVELOPED VS. PSAT ROUTINES)

Case	Author-developed routines						PSAT routines					
	CNR code			Compromise CLF code			PSAT - PI mode			PSAT - LP mode		
	$\lambda_{max}$ [-]	points	time [s]	$\lambda_{max}$ [-]	points	time [s]	$\lambda_{max}$ [-]	points	time [s]	$\lambda_{max}$ [-]	points	time [s]
IEEE9	2.485393	74	0.5460	2.485382	84	0.2964	2.481220	7	0.2093	2.482000	13	0.3241
IEEE13	4.400579	148	0.6708	4.400577	112	0.3120	4.390420	13	0.3292	4.399570	20	0.4832
IEEE14	4.060253	137	0.8268	4.060252	92	0.3276	4.060100	18	0.4098	4.059420	19	0.4939
IEEE24	2.279398	61	0.6396	2.279398	58	0.2496	2.277550	10	0.2600	2.278670	16	0.4313
IEEE30	2.958815	88	0.8112	2.958814	57	0.2964	2.958550	16	0.8761	2.958250	20	1.5023
IEEE35	2.888962	91	0.6864	2.888950	107	0.3432	2.872940	16	1.1242	2.878420	10	0.2940
IEEE39	1.999203	57	0.7644	1.999202	30	0.2184	1.999110	11	0.2932	1.997840	12	0.3692
IEEE57	1.892091	47	0.8892	1.892089	92	0.4836	1.891920	12	0.9089	1.892090	26	3.9090
IEEE118	3.187128	100	1.6536	3.187128	66	0.5772	3.187100	613	19.1693	3.187120	82	19.7464

X. DETERMINATION OF CRITICAL NETWORK REGIONS IN TERMS OF VOLTAGE STABILITY

This approach is demonstrated on the 59-bus test network which is a simplified 14-generator model of the South-East Australian Power system [21]. Peak load conditions (case C: total base-case generation/load of 25.43/24.8 GW) were selected as the most attractive for the voltage stability study. Neither G-S nor standard N-R method were able to provide base-case load flow solution. Therefore, the use of stability techniques in the first corrector step is of high importance.

Total of 41 buses were activated for load/generation increase (L+G scenario) with step size setting of  $2.5 \times 10^{-2} / 6.25 \times 10^{-3}$  to achieve fair compromise between the accuracy and the CPU time. Total number of 153 stable/unstable V-P points were calculated in less than 1.17 seconds. Found value of  $\lambda_{max}$  was 1.2518 [-] for which all network buses remained inside their permitted  $\pm 10\%$  voltage tolerance.

In Fig. 11, the V-P curves for PQ bus No. 43 and PV bus No. 46 are shown. For the latter, the selected PV bus maintained its voltage control capability up to loadability of approx. 1.2 [-]. Then, it was switched to PQ and a sharp point on the V-P curve emerged. At loadability of 1.24 [-], another PV network bus was switched to PQ (2<sup>nd</sup> sharp point arisen).

In Fig. 12, relative reactive power reserve of the network is drawn. The decrease by approx. 63 percent between the base case and the singular point is clearly visible. Thus, the system still provides voltage-var control. In other cases, however, zero var reserve is usually hit far before the singular point.

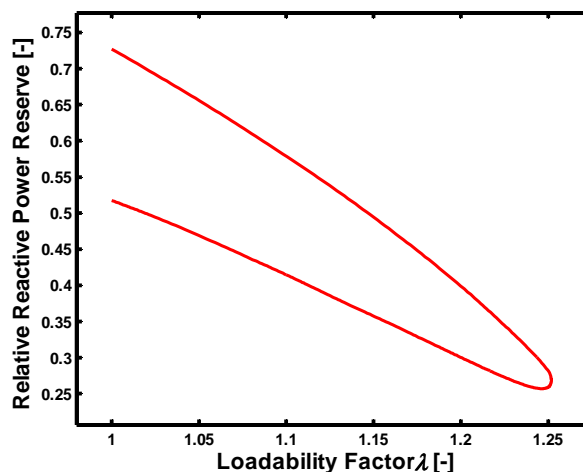


Fig. 12. Relative level of reactive power reserve [15].

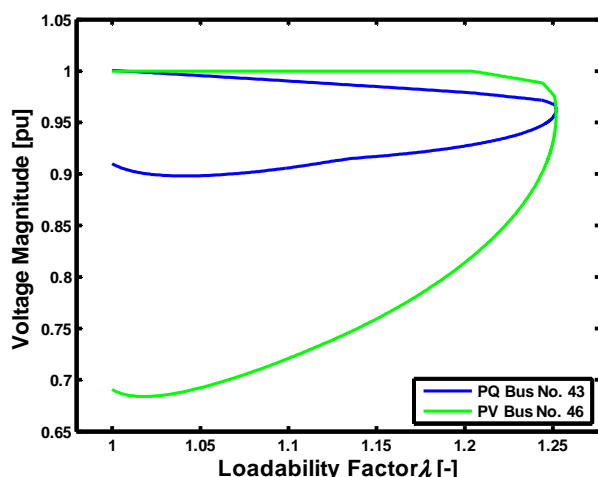


Fig. 11. V-P curves for selected PV/PQ network buses [15].

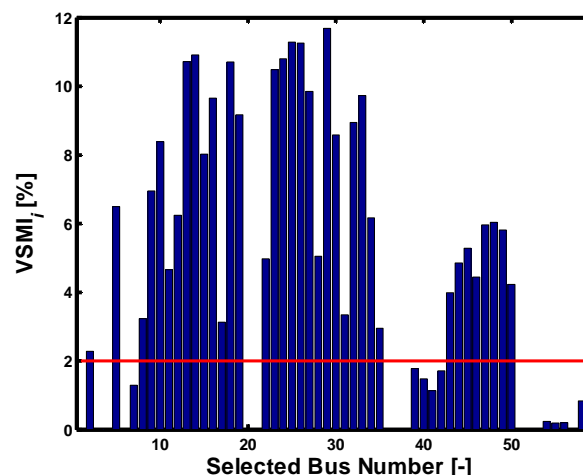


Fig. 13. Voltage stability margin indices - bus conditions [15].

In Figs. 13 and 14,  $VSMI_i/VSMI_{ik}$  indices are presented for each network bus/branch, respectively. In the former, blank columns belong to those PV buses (incl. the slack bus) which still provide voltage-var control. Buses No. 7, 39-42, 54-56 and 58 were found the most critical with  $VSMI_i$  values below security level of 2 %.

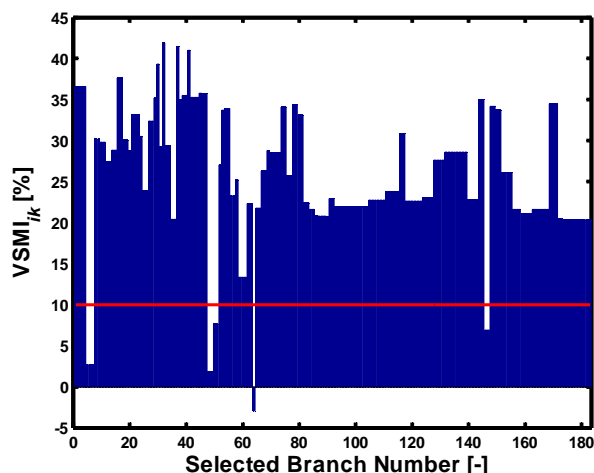


Fig. 14. Voltage stability margin indices - branch conditions [15].

The most critical  $VSMI_{ik}$  values were found for branches No. 5-7 (buses No. 2-28), 48-51 (buses No. 28-29 and 29-30), 64 (buses No. 41-42) and 146-147 (buses No. 24-30).

Finally, sensitivity study was performed to show voltage-load sensitive network areas. In these regions, protective measures should be applied to prevent/minimize the effects of possible voltage instabilities. The  $VSF_i$  values were calculated for each non-slack network bus using the  $dV$  vector of the predictor in close vicinity to the singular point. System buses with the highest  $VSF_i$  values are shown in Table III.

TABLE III. HIGHLY VOLTAGE-LOAD SENSITIVE NETWORK BUSES

bus	48	47	49	44	46	50
$VSF_i$ [-]	0.106	0.106	0.105	0.099	0.096	0.092
bus	35	45	7	43	42	39
$VSF_i$ [-]	0.091	0.090	0.070	0.027	0.018	0.016

Network scheme along with highlighted voltage-weak areas (high  $VSF_i$  values) and critical buses/branches (low  $VSMI_i$  and  $VSMI_{ik}$  values) is shown in Fig. 15. Voltage-weak areas were structured in zones 1 (highest sensitivity) to 3 (high sensitivity) to easily locate the epicentre of possible voltage-sensitivity problems.

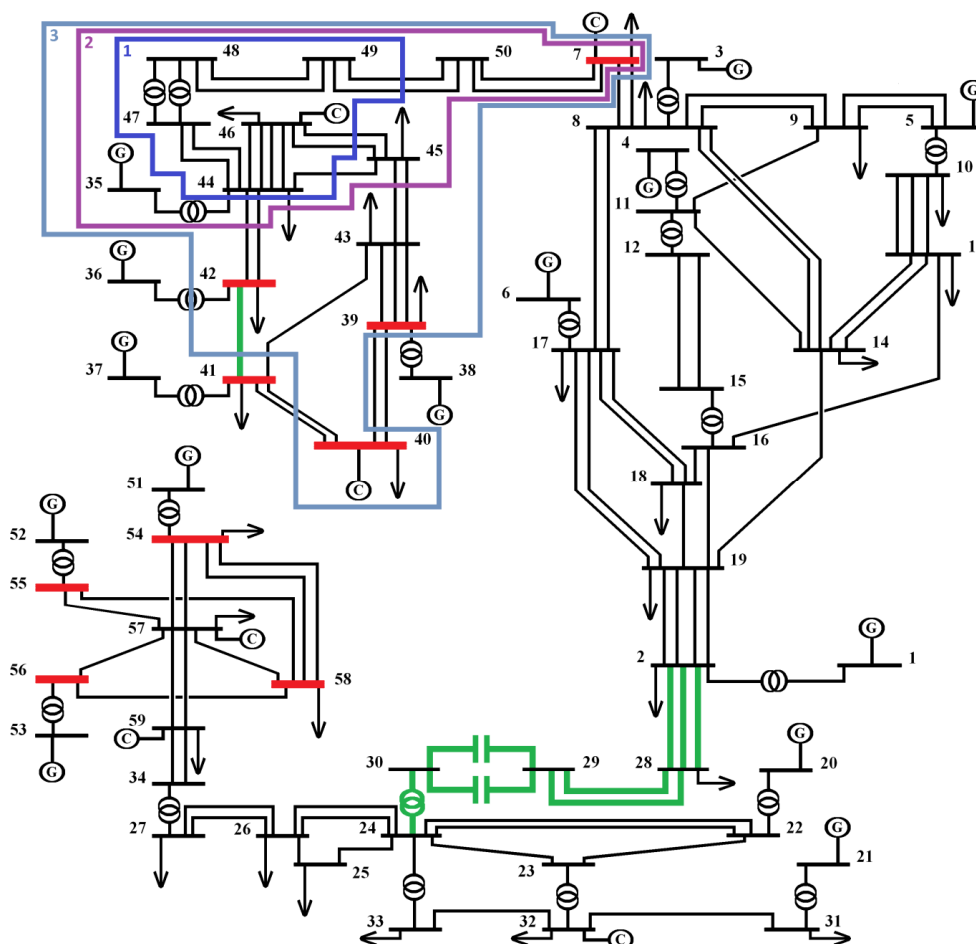


Fig. 15. Network scheme with highlighted critical buses/branches/areas.

Following corrective strategies are proposed for improving the voltage stability situation: 1) Connect synchronous condensers/generators and/or apply load-shedding in critical buses located in weak network areas (i.e. those with lowest  $VSMI_i$  and highest  $VSF_i$  values). 2) Use broader var limits and higher voltage magnitudes in PV buses inside or close to weak areas. 3) Disconnect all shunt inductors. 4) Activate synchronous condensers or shunt capacitors to buses with the lowest  $VSMI_i$  values outside the highly sensitive regions.

Individual corrective actions can be mostly applied only when approaching the singular point. They are meaningful only with respect to the region of viable voltage values and reasonable branch loadings. Proposed corrective process is to implement each corrective action individually, repeat the voltage stability analysis of the system, locate new weak system regions and activate the next suitable correction. Thus, multiple corrective strategies can be prepared. The most suitable would be the one with the best compromise between possible stability improvements and acquisition/operational costs.

For more details about this methodology and this case study see [15].

#### XI. DETERMINATION OF SHORTEST DISTANCE TO VOLTAGE INSTABILITY

The SDVI approach with the modified CNR method was applied on a set of 26 real medium-sized and larger distribution power systems between 7 and 794 buses. In each case study, the PQ buses with non-zero active power load were activated for the analysis. All eigenvalues with relevant left eigenvectors were computed at the end of each loading scenario, the real eigenvalue with minimum magnitude was found and used to determine the next loading increase direction. As the outputs, two matrices were always generated. The former contains the distance to voltage instability, total active/reactive system loading and the smallest eigenvalue of the Jacobian for each loading scenario taken. The latter consists of the minimum MW/MVAr increments in all network buses for reaching voltage instability.

Except for the CNR method, the most time-consuming part of this analysis was the computation of all eigenvalues and left eigenvectors for the singular non-sparse Jacobian (function 'eig') along with locating the smallest eigenvalue. Code upgrades were further implemented to compute only the one key eigenvalue and left eigenvector of the sparse Jacobian (via 'eigs(Jacobi.',1,'SM')') for the new direction vector. When comparing both code versions (eig vs. eigs functions) in terms of CPU time and solution accuracy, significant CPU time savings were achieved by the latter with only slightly lower precision - see Fig. 16. Time savings ranged between 8.8 percent for smaller and 80.25 percent for larger systems. After the acceleration process, maximum CPU time needed for meeting given convergence criterion of  $1 \times 10^{-8}$  was 44.05 seconds.

Note: All the testings were performed at IntelCore i3 CPU 2.53 GHz/3.8 GB RAM computer station.

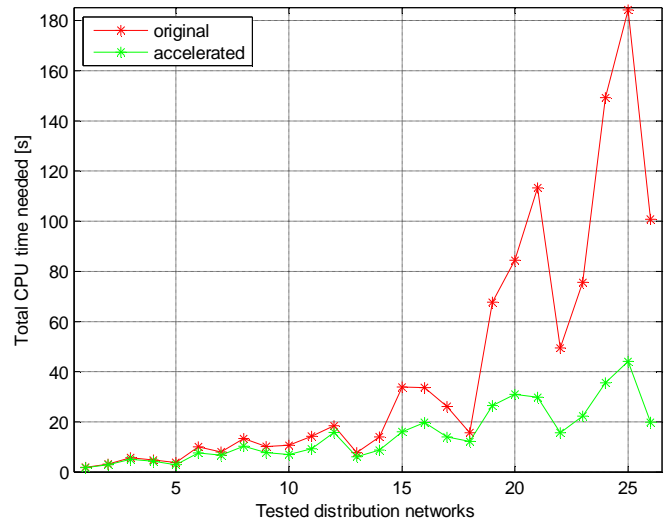


Fig. 16. Comparison of CPU times for original (eig) and accelerated (eigs) code versions. Note: Networks (with their sizes) are sorted upwards.

Comparison between the initial (uniform) and the minimum (critical) P/Q load increase direction was performed in terms of the distance to voltage instability. As presented in Fig. 17, significant decreases between 9.61 and 91.21 percent were obtained.

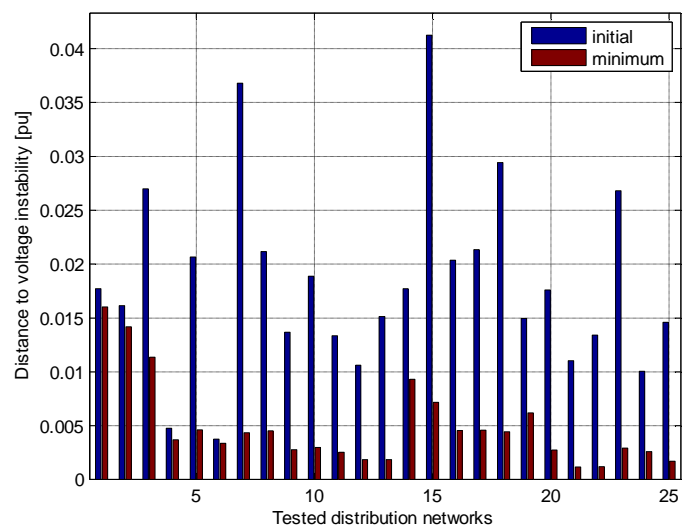


Fig. 17. Comparison of initial and minimum distances to instability for 25 examined networks

Detailed study is provided for the 19-bus 110/22 kV distribution network [22] of the western part of Czech Republic - see Fig. 18. It includes the connection to the superior system via the shunt conductance and susceptance in the slack bus.

The goal is to find minimum MW/MVAr increments in load buses No. 6, 7, 8, 10, 11, 14, 15, 18 and 19 for the base case of -134.1 MW and -39.9 MVAr to reach voltage instability. Uniform initial load increase was applied for active/reactive power loads. In Table IV., searching process

for finding the locally minimum distance to voltage instability is presented.

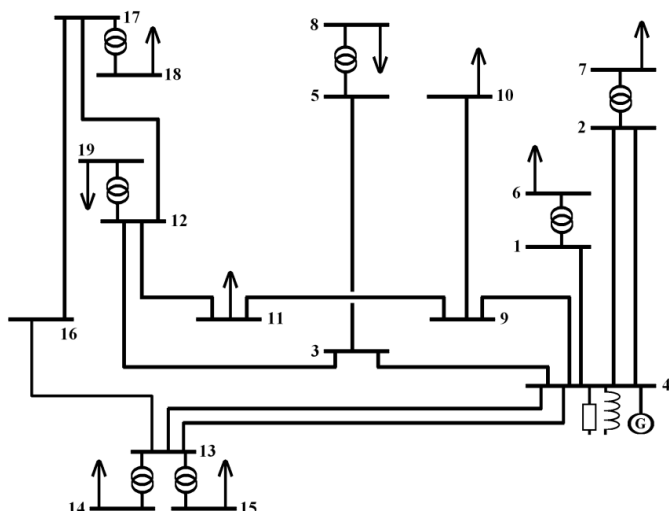


Fig. 18. Scheme of the 19-bus 110/22 distribution network (Distribution Pilsen - South)

TABLE IV. SEARCHING PROCESS FOR LOCAL MINIMUM DISTANCE TO VOLTAGE INSTABILITY

loading scenario number	distance to instability	total $P_L$ (singular point)	total $Q_L$ (singular point)	min eigvalue
1	1.26659	-4.02784	-3.08584	1.57e-4
2	0.39126	-1.51583	-0.74903	-1.46e-4
3	0.38566	-1.46315	-0.76480	7.93e-5
4	0.38455	-1.43958	-0.77070	9.69e-5
5	0.38432	-1.42883	-0.77315	1.05e-4
6	0.38427	-1.42390	-0.77422	-1.21e-4
7	0.38426	-1.42163	-0.77470	-1.53e-4
8	0.38426	-1.42058	-0.77493	1.60e-4
9	0.38426	-1.42011	-0.77502	4.87e-5
10	0.38426	-1.41988	-0.77507	1.30e-4
11	0.38426	-1.41978	-0.77509	-1.19e-4
12	0.38426	-1.41973	-0.77510	9.36e-5

As can be seen, initial uniform loading leads to excessively optimistic distance to voltage instability (about 1.2666 pu, i.e. increase of about 268.6842 MW/MVAr). The entire searching process converges relatively quickly where the solution does not change too much after the third loading scenario. Under the critical loading increase, much lower distance to voltage instability is obtained (about 0.3843 pu, i.e. decrease of 69.66 percent). At this point, only increase of 7.87 MW and 37.61 MVAr to the base-case loading leads to instability.

Critical MW/MVAr bus increments for reaching voltage instability are surprisingly bound only with bus No. 6 which may still withstand such load increase during real operating conditions - see Fig. 19.

In all performed studies, uniform initial load increase was always applied. This means that both active/reactive power

loads in all network buses were increased equally (i.e. under -135 degrees in the P-Q plane). Under other initial directions, different shortest distance to instability and critical loading scenarios can be obtained. Therefore, historically or technically reasonable loading scenario for the network operation must be always chosen at the beginning of the analysis.

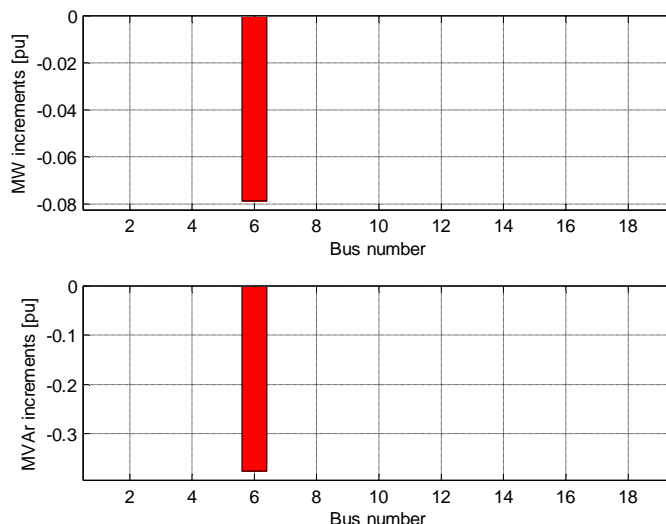


Fig. 19. Minimum MW/MVAr bus increments

Based on results above, it is necessary to focus on finding the minimum distance to instability when evaluating voltage stability margins of the network since uniform load increases may provide reasonable but too optimistic results. Then, the rationality of the critical loading scenario obtained should be evaluated.

From all case studies follows that no significant changes in the solution are achieved after the third iteration (i.e. loading scenario found). Thus, computation time of this analysis could be pushed below 20 seconds. Therefore, applied methodology for voltage stability evaluation is not suitable for real-time decision-making system processes. However, it could be helpful when working with 1-minute forecasted operation schemes of the network and estimated load changes in individual buses (for initial loading increase directions).

## XII. CONCLUSIONS

Nowadays, voltage collapse and islanding scenarios have been evaluated as one of the most serious problems in electric power system operation and control worldwide. This can be documented on large number of extensive power outages around the world which were strongly connected to material and human losses. Therefore, highly robust algorithms for fast and reliable detection of voltage instabilities in currently operated power systems must be of the highest priority.

In this paper, both CNR and CLF codes were implemented and thoroughly tested on a broad range of test power systems in MATLAB environment for solving voltage stability problems. Various stability techniques, step size approaches and numerical settings were applied and used to upgrade their performance in order to find the algorithm with fair

compromise between calculation speed and solution accuracy. Their final results were compared to outputs obtained from PSAT. The studies imply that the technique with the best combination of precision level and CPU time requirements is the CLF algorithm with compromise step size settings.

Optimized CLF code was further applied for locating weak network buses/branches/areas in terms of voltage stability. By implementing various voltage stability indices and sensitivity factors, comprehensive picture about the network operation can be obtained and used for the implementation of particular corrective or remedial actions. These actions must be applied individually to build a set of possible corrective strategies. When the low voltage stability situation appears, the one with fair compromise between economical and technical criteria should be employed.

Modified CNR code was implemented in the SDVI approach for finding the critical loading scenario (i.e. the one with minimum load increase) which causes the network to reach the voltage collapse. In this procedure, it is important to specify reasonable initial loading scenario based on operator's forecasted or predicted data. Unlike the uniform load increase, significantly smaller distances to voltage instability (and thus, more pessimistic solutions) are obtained.

However, presented techniques are the best to be used for off-line planning and development studies of electric power systems only. For real-time evaluations of system's voltage stability, more robust algorithms with minimized numbers of stable V-P points are to be developed. Therefore, follow-up research activities will be concentrated especially on this area of interest.

### XIII. ACKNOWLEDGMENT

This paper was supported by Technology Agency of the Czech Republic (TACR), project No. TA01020865 and by student science projects SGS-2012-047 and SGS-2013-029.

### REFERENCES

- [1] P. Kundur, *Power System Stability and Control*. McGraw-Hill, 1994.
- [2] C. Canizares, A. J. Conejo, and A. G. Exposito, *Electric Energy Systems: Analysis and Operation*. CRC Press, 2008.
- [3] V. Ajjarapu, *Computational Techniques for Voltage Stability Assessment and Control*. Springer, 2006.
- [4] I. Dobson, T. V. Cutsem, C. Vournas, C. L. DeMarco, M. Venkatasubramanian, T. Overbye, and C. A. Canizares, "Voltage Stability Assessment: Concepts, Practices and Tools," *IEEE-PES*, 2002.
- [5] J. H. Chow, F. F. Wu, and J. A. Momoh, *Applied Mathematics for Restructured Electric Power Systems - Optimization, Control and Computational Intelligence*. Springer, 2005.
- [6] T. Ratniyomchai, and T. Kulworawanichpong, "Evaluation of Voltage Stability Indices by Using Monte Carlo Simulation," *Proceedings of the 4th IASME / WSEAS International Conference on ENERGY & ENVIRONMENT (EE'09)*, pp. 297-302, 2009.
- [7] A. Zare, and A. Kazemi, "Proposing a Novel Method for Analyzing Static Voltage Stability," *Selected papers from the WSEAS conference of Recent Advances in Systems Engineering and Applied Mathematics*, pp. 146-151, 2008.
- [8] Q. Zhang, and C. Chen, "Wu Elimination Method Applied in Analytical Solution of the Power System Voltage Stability," *Proceedings of the 8th WSEAS International Conference on Systems Theory and Scientific Computation (ISTASC'08)*, pp. 255-259, 2008.
- [9] G. Negi, A.K. Swami, S.K. Goel, and A. Srivastava, "Assessment and Improvement of Voltage Stability using ANN Architecture," *Proceedings of the 7th WSEAS International Conference on Electric Power Systems, High Voltages, Electric Machines (POWER'07)*, pp. 203-208, 2007.
- [10] A.R. Minhat, I. Musirin, M. M. Othman, and M. K. Idris, "Assessment of Maximum Loadability Point for Static Voltage Stability Studies Using Evolutionary Programming," *Proceedings of the 6th WSEAS International Conference on Applications of Electrical Engineering (AEE'07)*, pp. 96-101, 2007.
- [11] M. J. Chen, B. Wu, and C. Chen, "Determination of Shortest Distance to Voltage Instability with Particle Swarm Optimization Algorithm," *European Transactions on Electrical Power*, vol. 19, pp. 1109-1117, 2008.
- [12] Y. Jie, L. Hong-Zhong, W. Cheng-Min, and J. Yi-Xiong, "A hybrid way to construct static voltage stability region based on combining loop current with node voltage," *Proceedings of the 7th WSEAS International Conference on Mathematical Methods and Computational Techniques in Electrical Engineering (MMACTEE'05)*, pp. 300-304, 2005.
- [13] A. Augugliaro, L. Dusonchet, S. Favuzza, and S. Mangione, "An Improved Method for Determining Voltage Collapse Proximity of Radial Distribution Networks," *Proceedings of the 5th WSEAS International Conference on Power Systems and Electromagnetic Compatibility (PSE'05)*, pp. 78-84, 2005.
- [14] M. Crow, *Computational Methods for Electric Power Systems*. CRC Press, 2002.
- [15] J. Veleba, "Application of Continuation Load Flow Analysis for Voltage Collapse Prevention," *Journal Acta Technica*, vol. 57, pp. 143-163, 2012.
- [16] P. Zhu, *Performance Investigation of Voltage Stability Analysis Methods*. Ph.D. thesis, Brunel University of West London, 2008.
- [17] Homepage of PSAT. [Online]. Available: <http://www3.uclm.es/profesorado/federico.milano/psat.htm>. [Accessed: 3 Mar. 2013].
- [18] Homepage of MATPOWER. [Online]. Available: [www.pserc.cornell.edu/matpower/](http://www.pserc.cornell.edu/matpower/). [Accessed: 23 Dec. 2012].
- [19] D. S. Popović, "Impact of Secondary Voltage Control on Voltage Stability," *Electric Power Systems Research* 40, vol. 40, pp. 51-62, 1997.
- [20] J. Veleba, "Acceleration and Stability Techniques for Conventional Numerical Methods in Load Flow Analysis," *Proceedings of ELEN conference*, pp. 1-10, 2010.
- [21] Simplified 14-generator model of the SE Australian Power system. [Online]. Available: [http://www.eleceng.adelaide.edu.au/Groups/PCON/PowerSystems/IEEE/BenchmarkData/Simplified\\_14-Gen\\_System\\_Rev3\\_20100701.pdf](http://www.eleceng.adelaide.edu.au/Groups/PCON/PowerSystems/IEEE/BenchmarkData/Simplified_14-Gen_System_Rev3_20100701.pdf). [Accessed: 2 Nov. 2011].
- [22] P. Šilhán, *Modelování a řízení přenosové soustavy*. Ph.D. thesis, University of West Bohemia in Pilsen, 2008.